Article:
Torres-Salomao, L.A., Mahfouf, M., El-Samahy, E. et al. (2016) Psycho-Physiologically-Based Real Time Adaptive General Type 2 Fuzzy Modelling and Self-Organising Control of Operator's Performance Undertaking a Cognitive Task. IEEE Transactions on Fuzzy Systems. ISSN: 1063-6706

https://doi.org/10.1109/TFUZZ.2016.2598363

This article has been accepted for publication in a future issue of this journal, but has not been fully edited. Content may change prior to final publication. Citation information: DOI 10.1109/TFUZZ.2016.2598363, IEEE Transactions on Fuzzy Systems

Psycho-Physiologically-Based Real Time Adaptive General Type 2 Fuzzy Modelling and Self-Organising Control of Operator's Performance Undertaking a Cognitive Task

Luis A. Torres-Salomao, *Member IEEE*, Mahdi Mahfouf, Emad El-Samahy and Ching-Hua Ting

***Abstract*—This paper presents a new modelling and control fuzzy-based framework validated with real-time experiments on human participants experiencing stress via mental arithmetic cognitive tasks identified through psycho-physiological markers. The ultimate aim of the modelling/control framework is to prevent performance breakdown in human-computer interactive systems with a special focus on human performance. Two designed modelling/control experiments which consist of carrying-out arithmetic operations of varying difficulty levels were performed by 10 participants (operators) in the study. With this new technique, modelling is achieved through a new adaptive, self-organizing and interpretable modelling framework based on General Type-2 Fuzzy sets. This framework is able to learn in real-time through the implementation of a re-structured performance-learning algorithm that identifies important features in the data without the need for prior training. The information learnt by the model is later exploited via an Energy Model Based Controller that infers adequate control actions by changing the difficulty level of the arithmetic operations in the human-computer-interaction system; these actions being based on the most current psycho-physiological state of the subject under study. The real-time implementation of the proposed modelling and control configurations for the human-machine-interaction under study shows superior performance as compared to other forms of modelling and control, with minimal intervention in**

Manuscript received October 30, 2015. The work of L. A. Torres-Salomao was supported by the Mexican National Science Council (CONACyT), Mexico city, Mexico.

L. A. Torres-Salomao and M. Mahfouf are with the Department of Automatic Control and Systems Engineering, The University of Sheffield, Sheffield, S13DJ, United Kingdom (e-mail: latsalomao@ieee.org; m.mahfouf@sheffield.ac.uk).

E. El-Samahy is with Biomedical Engineering Department, Military Technical College, Cairo, Egypt (email: e.elsamahy@gmail.com)

C.-H. Ting is with Department of Mechanical and Energy Engineering, National Chiayi University, Chiayi, 60004, Taiwan (email: cting@mail.ncyu.edu.tw)

terms of model re-training or parameter re-tuning to deal with uncertainties, disturbances and inter/intra-subject parameter variability.

***Index Terms*—Type 2 fuzzy sets, human machine interaction, psycho-physiological markers, mental stress, modelling, control, real time, adaptive.**

I. Introduction

Today's computer systems have changed the way we think and have allowed for path-opening to many paradigm changes in diverse areas. We constantly rely on these computer-based systems and as a result we delegate to them many of the other activities we took responsibility for not so long ago.

Thanks to this revolutionary computational power, automation systems are finding their way into all devices thinkable, ranging from consumer-friendly electronic devices to very specialized equipment, hence breaking the barriers of science, e.g. the hadron collider at CERN, or the electronic devices for space exploration [1].

For the community working with control systems this has meant a shift from traditional approaches for modelling and control mainly based on mathematics and laws of nature, towards data-driven approaches that rely on simple 'mining' algorithms powered by very fast and intensive computations. Many techniques, such as artificial neural networks and fuzzy logic systems, exist that take advantage of this change in paradigm facilitated by the advancement in computational technologies.

There are however many barriers yet to be broken and the exploration of Human-Machine Interaction (HMI) systems is one of them. As we strive to automate ever more of the machines we interact with it is also very important to acknowledge their psychological and physiological effect on us in order to completely understand our interaction with them. The role of the human should be given a special attention [2]. Though albeit representing a very 'tricky' task since the variables and features in these biological

systems are not fully understood and vary significantly under similar conditions given their high level of complexity.

For safety critical systems (e.g. nuclear power plants), the adaptive capabilities and reasoning of human operators are often required to play an intrinsic role in the HMI system that cannot be (partially or fully) automated [3]. The decision on which tasks to automate and which tasks to leave to the human operator is indeed concomitantly important and challenging [4], and the mental and physical state of the operator should be given special considerations [1, 5, 6].

Cautiously but confidently we find ourselves with ever more advanced and intelligent algorithms and techniques that are capable to self-adapt, self-organise and evolve as the systems they are called upon to monitor are themselves evolving. Data-driven automatic approaches are now able to begin to understand HMI systems by extracting meaningful features. A selection of such intelligent algorithms can be found in [7-15]. Most of these algorithms focus on learning in an off-line configuration [7, 8, 11-15], and lack highly desirable online adaptive features needed for HMI systems. The works presented in [9, 10] address real-time adaptive learning algorithms. In [10] an online learning system capable of generating and deleting rules for an adaptive fuzzy-neural control system has been presented and tested. A further development into a self-organizing adaptive system is presented in [9]. In this system, rules are added, replaced, deleted and the parameters of a Takagi-Sugeno fuzzy structure are recursively adapted, achieving identification and tracking control. Both works [9, 10], present innovative approaches for the design of online, self-organizing, adaptive and semi-interpretable modelling and control applied to non-linear systems. However, they do not provide a robust enough framework capable of truly describing and weighting uncertainty for systems with inter- and intra-parameter variability.

The techniques in [7-15] (i.e., neural network approaches, support vector machines, clustering approaches, fuzzy logic systems), lack one or more of the following highly desirable features for HMI systems:

- Adaptation: widely understood as the ability to restructure themselves in real-time in response to

changes in the system they monitor.

- Handling of uncertainty: their ability to handle ill-defined systems with un-modelled dynamics.
- Interpretability: to be able to easily translate what these models learn into rules understandable by humans.
- Self-organization: their ability to learn by themselves and in real-time without the need for a training phase.

As will be introduced in the development of this work, in order to close the loop of the HMI system under study (of operators performing mentally stressful arithmetic operations) it is necessary to address the above features to construct a fully functional system.

The paper is organized as follows: Section II presents the Mental Arithmetic operations based experiment and evidence of its transferability to other HMI systems. Section III deals with the various features relating to the psycho-physiological signals used for this work. In Section IV a new Adaptive General Type-2 Fuzzy C-Means (A-GT2-FCM) modelling system is presented. Section V addresses an Energy Model Based Controller (E-MBC) design procedure for decision-making. In Sections VI and VII results of the real-time experiments under the proposed modelling/control framework are compared to a benchmark Adaptive Neuro-Fuzzy Inference System (ANFIS) modelling and heuristic control. Conclusions relating to the claims made in this paper about the modelling and control framework for the HMI are drawn in the last section.

II. Mental Arithmetic Operations Experiment

A. Experimental background

Mental Arithmetic (MA) was selected as the task to induce mental stress in the participants of this study. This task was selected following extensive research whereby several experimental frameworks were investigated and analysed [1]. The studied experimental frameworks included: the operation of a computer simulated automation-enhanced Cabin Air Management System (aCAMS) [3, 16], Stroop Colour Word

This article has been accepted for publication in a future issue of this journal, but has not been fully edited. Content may change prior to final publication. Citation information: DOI 10.1109/TFUZZ.2016.2598363, IEEE Transactions on Fuzzy Systems

Testing, Mental Arithmetic (MA) operations, cold presser test, and coin stacking task, among many others [17-22].

The selected task in an experiment to induce mental stress is as important as the measured psycho-physiological markers themselves [1]. Because of this specific reason, it is very important to analyse the task effectiveness in producing a cognitive load in the participant. Additionally, it is important to consider other aspects such as:

1. Its reproducibility; MA is a fully reproducible experiment, mainly due to its simplicity.

2. Its representativeness of real-life Human Machine Interaction (HMI) systems. Experimental frameworks that are more accurate descriptions of real-life HMI systems have been performed in the past with the operation of transport vehicles [20, 21] or with complex computer simulations like in [3, 16]. Despite their match to the real world, they are usually difficult to reproduce and/or require training of participants. It is also important to note that economic costs are also a constraint in these cases. MA is intuitive and requires no training, making it cheap to run. In [1, 18, 19, 22] the effect on commonly used psycho-physiological markers show that MA produces similar effects to the ones present in other experiments such as those described in [3, 16] with the aCAMS simulator.

3. Its validation property to ensure it is comparable with state-of-the-art research in the area; MA operations have been successfully used in the past in [1, 18, 19, 22]. When compared with the commonly used Stroop Colour Word Testing, studies presented in [17-19] in fact position MA as a better mental stressor.

B. Hardware and software for experiment

For the production of psycho-physiological markers, three main measurements were taken: electro-encephalogram (EEG), electro-cardiogram (ECG) and pupil size. EEG and ECG were acquired using the ActiveTwo System by BioSemi. Electro-oculogram measurements were also taken for future experiments on EEG noise recovery. The experimental framework utilised for the acquisition of these signals was the same as the one presented in [3, 16]. With regards to the pupil size acquisition, a

This article has been accepted for publication in a future issue of this journal, but has not been fully edited. Content may change prior to final publication. Citation information: DOI 10.1109/TFUZZ.2016.2598363, IEEE Transactions on Fuzzy Systems

GAZEPOINT GP3 Eye Tracker was used similarly as in [1, 22]. Fig. 1 depicts a participant in the study while connected to the acquisition system.

Fig. 1. Picture of a participant in the study while connected to the ActiveTwo Biosemi box for acquisition of EEG, ECG and EOG. Pupil size was acquired with the GAZEPOINT GP3 Eye Tracker.

For the MA experiment, a graphical user interface (GUI) was designed in MATLAB®. Data acquisition was carried-out for EEG, ECG and EOG with this software over TCP/IP protocol, communicating with the ActiView LabVIEW™-based software provided by BioSemi. The signals produced with this hardware were acquired in a decimated 256 Hz frequency. For the pupil size, communication was also achieved through TCP/IP with the use of the GAZEPOINT GP3 Eye Tracker server on a 60 Hz native frequency [1]. The GUI also supported, in addition to the acquisition of these signals, the experimental deployment of arithmetic operations at controlled intervals and with varying difficulty levels, the psycho-physiological markers real-time computation, the adaptive real-time model algorithm and the model-based controllers. Fig. 2 shows an image of the user-end GUI designed in MATLAB® for the MA experiment.

C. Configuration of experiment

Three basic configurations of experiments were performed. For the first two configurations (Modelling Experiments 1 and 2), the psycho-physiological markers were computed and used as inputs to the Adaptive General Type-2 Fuzzy C-Means (A-GT2-FCM) modelling framework and to participant-specific Adaptive Neuro-Fuzzy Inference Systems (ANFIS) modelling framework [23] (which will be later used for

This article has been accepted for publication in a future issue of this journal, but has not been fully edited. Content may change prior to final publication. Citation information: DOI 10.1109/TFUZZ.2016.2598363, IEEE Transactions on Fuzzy Systems

comparison) for the production of Predicted Accuracy Performance (PAP). The last configuration (Control Experiments) added the designed Energy Model-Based Controller (E-MBC) and participant-specific ANFIS Controllers (ANFIS-C) for this HMI system (see Section VI).

Modelling Experiments 1 (ME-1) and 2 (ME-2) consisted of four (4) phases of 180 s each and were performed one after the other in the same session. For ME-1 these 4 consecutive phases were of incremental difficulty levels (*DL*), evolving from *DL=1* (relatively easy) to *DL=4* (most difficult). *DL=1* consisted of summations of two random numbers of 1 to 2 digits with participants given 10 s to provide an answer (see Fig. 2*(b)*), *DL=2* was similar to *DL=1* with the difference that participants had only 5 s to provide an answer. *DL=3* and *DL=4* followed this same pattern but with numbers of 2 to 3 digits and with participants having 10 s and 5 s to provide an answer respectively (see Fig. 2*(c)*). All participants experienced a decreased performance at *DL=4*. For ME-2 the difficulty level phases were 'scrambled'. The order of the difficulty levels in ME-2 was changed to block the effect of fatigue and to evaluate the order change effect in the psycho-physiological markers. Fig. 3 is a graph representing the difficulty levels plotted against time for ME-1 and ME-2.

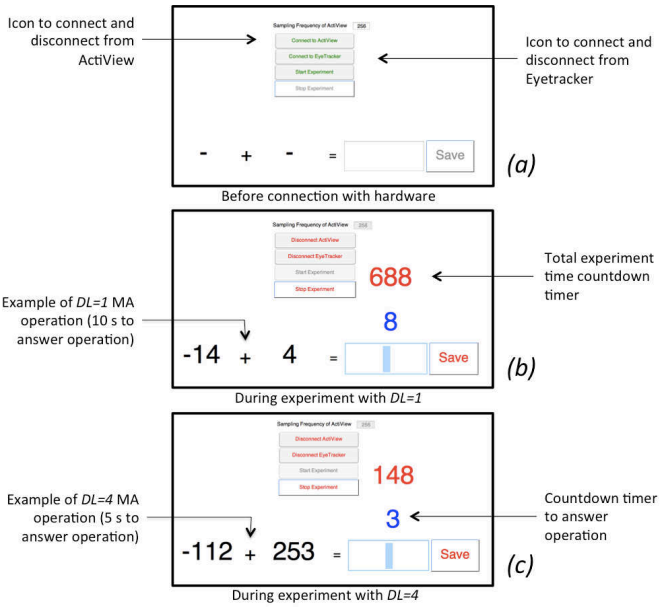

Fig. 2. Graphical user interface software designed in MATLAB® for the MA experiment. (a) Shows the GUI before the hardware is connected (ActiView box and eye-tracker). (b) Shows the GUI during the experiment on *DL*=1. (c) Shows the GUI during the experiment on *DL*=4.

This article has been accepted for publication in a future issue of this journal, but has not been fully edited. Content may change prior to final publication. Citation information: DOI 10.1109/TFUZZ.2016.2598363, IEEE Transactions on Fuzzy Systems

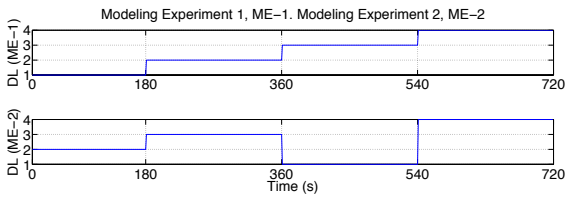

Fig. 3. Difficulty level for Modelling Experiment 1 (increasing difficulty), top plot. Modelling Experiment 2 (scrambled difficulty), bottom plot.

III. Psycho-Physiological Markers

A. Selection and calculation of psycho-physiological markers

The acquisition of psycho-physiological signals from the body surface, should provide meaningful responses to stressful events [24]. This way, it is possible to use these signals to identify the presence of mental and/or physical stressors.

Mental stress has been identified in the past through the acquisition of cardiovascular bodily signals such as Heart Rate Variability (HRV) [21, 25, 26]. Cognitive processes (e.g., planning, attention, reasoning, problem solving and decision making) also correlate strongly with mental stress [27] and are assumed to emanate from the activity of the prefrontal cortex area of the brain. Midline theta activity in this region through Gevins' (1997) Task Load Index (TLI) [28, 29] was found to correlate with mental stress in complex task environments [30, 31].

A previous study performed in the 'Human Performance Laboratory' at the University of Sheffield found evidence of sufficient correlation between HRV and TLI with a performance index calculated from the aCAMS simulation model [3, 16].

Pupil size change and pupil size change acceleration have been linked with cognitive load in human computer interaction studies for Stroop Colour Word Testing experiments in [32-34]. More recently, a study performed also at the 'Human Performance Laboratory' used these pupil size markers together with Heart-Rate (HR) in a MA experiment [22] following a statistical correlation study of incremental levels of mental stress to evaluate the power of this marker in [1]. The study in [1] linked the Pupil Diameter Marker

(PDM) with mental stress originated from the same MA experimental configuration as the one presented in this work.

This work combines five key and previously successful markers for the detection of mental stress in a MA experiment. Namely, Heart Rate Variability 1 (HRV_1), Heart Rate Variability 2 (HRV_2), Task Load Index 1 (TLI_1), Task Load Index 2 (TLI_2) and Pupil Diameter Marker (PDM). As already stated, every MA experiment lasted for 720 s. All markers were calculated with data collected within windows of 30 s and shifted every 1 s to obtain a total of 690 marker data samples.

The computation process relating to the cardiovascular indices (e.g., HRV) was derived from the power spectrum analysis of the cardiac interval [16]. HRV_1 is a marker that represents the 0.1 Hz component (e.g., in the frequency range from 0.07 Hz to 0.14 Hz) of the HR signal. For this work, it was calculated by averaging the power spectrum of HR collected during the 30 s period window. The marker HRV_2 was calculated as the ratio between the standard deviation over the mean value of the HR in the same 30 s window.

The TLI markers are based on the presence of high levels of theta activity at frontal midline sites and with attenuation of alpha power in parietal sites [16, 28]. These cognitive indices are defined as $TLI_1 = P_{\theta,Fz}/P_{\alpha,Pz}$ and $TLI_2 = P_{\theta,AFz}/P_{\alpha,CPz,POz}$, where P_θ and P_α relate to the theta-band (4 Hz to 7.5 Hz) and alpha-band (8 Hz to 12.5 Hz) powers of the EEG respectively. $P_{\theta,Fz}$ and $P_{\theta,AFz}$ represent the theta activities of the Fz and AFz electrode locations. The theta range power was calculated by averaging the power spectrum over the 30 s period. Similarly, $P_{\alpha,Pz}$ and $P_{\alpha,CPz,POz}$ are alpha activities of the Pz and the pool of CPz and POz electrode locations. [16]

The PDM calculation was performed following the hardware considerations presented in [1] with respect to blinking and relative distance from the eye-tracker. The pupil size, which is normally measured in pixels from the image captured by the eye-tracker, was averaged in the same 30 s period window.

This article has been accepted for publication in a future issue of this journal, but has not been fully edited. Content may change prior to final publication. Citation information: DOI 10.1109/TFUZZ.2016.2598363, IEEE Transactions on Fuzzy Systems

IV. Adaptive General Type-2 Fuzzy C-Means Modelling

Fuzzy logic is an established technique that is capable of handling uncertainties in the labelling of data in a transparent and simplified way by emulating the inference process that humans follow [35]. Fuzzy logic of Type-1 (T1FL) optimized with genetic algorithms was successfully used for the modelling and control of a HMI system for mental stress detection in [16]. The model presented in [16] was able to map input-output data with a general rule-base for all participants in the study. This successful result acknowledged the use of fuzzy systems for their ability to handle uncertainty in data to benefit the processing of predictions. However, a manual calibration was required before every experimental session due to the high variability in the scaling of the input psycho-physiological markers. This normalization process was required even when experiments were performed with the same participant, a fact derived from the important intra- and inter-parameter variability in humans.

Type-2 Fuzzy Logic (T2FL) in contrast, is a generalizing construct able to characterize uncertainties with an additional level of uncertainty to T1FL [36-41]. Despite the introduction of this powerful bi-dimensionally-structured mapping arrangement, its use is still problematic when the output processing is concerned [36, 41, 42]. This is the reason why most applications use the reduced Interval Type-2 (IT2) fuzzy representation that simplifies the output processing by making the secondary membership equal to 1 [36, 37, 43, 44]. In [3], an Interval Type-2 Fuzzy Logic (IT2FL) approach was used for the mental stress modelling of the data gathered in experiments presented in [16]. Results in [3] found more generalizing features than the T1FL version of [16], but retained the scaling problems of the T1FL experiment. Following these results it was quickly apparent that a more robust approach was needed to account for such parameter variability for a truly generalizing model. Because of the varying nature of the psycho-physiological markers used, and in order to acknowledge the time-dependent variations in the markers (e.g., due to fatigue or changes in temperature), a self-organizing and adaptive system capable of handling uncertainty was required. For these reasons, a new modelling framework named Adaptive General Type-2 Fuzzy C-Means (A-GT2-FCM) was devised to take advantage of the mapping capability of General

This article has been accepted for publication in a future issue of this journal, but has not been fully edited. Content may change prior to final publication. Citation information: DOI 10.1109/TFUZZ.2016.2598363, IEEE Transactions on Fuzzy Systems

Type-2 Fuzzy Logic (GT2FL) that can fully represent uncertainty [36-38, 40], the simplicity of Fuzzy C-Means (FCM) clustering algorithm to find relationships in data for rule generation [45], and the adaptive learning approach of negative Reinforcement Learning (RL) [46] to weight the uncertainty in the data for obtaining 'crisp' predictions. The idea behind A-GT2-FCM is one of a data-driven modelling framework capable of learning and storing information in real-time without the need for off-line training. The algorithm is based on a tri-dimensional rule-base *R* (equation (1)) whose first dimension (row) corresponds to the learned rules, its second dimension (column) corresponds to input and output variable mappings and the third dimension represents the uncertainty in the data. Part of the rule-base is the *SM* bi-dimensional matrix (see equation (2) below) that holds the information regarding the weighting of the modelled uncertainty:

$$R = \begin{cases} \begin{bmatrix} x_{111}, x_{121}, \dots, x_{1(d-1)1} : y_{11} \\ x_{211}, x_{221}, \dots, x_{2(d-1)1} : y_{21} \\ \vdots \\ x_{r11}, x_{r21}, \dots, x_{r(d-1)1} : y_{r1} \end{bmatrix} \\ \begin{bmatrix} x_{112}, x_{122}, \dots, x_{1(d-1)2} : y_{12} \\ x_{212}, x_{222}, \dots, x_{2(d-1)2} : y_{22} \\ \vdots \\ x_{r12}, x_{r22}, \dots, x_{r(d-1)2} : y_{r2} \end{bmatrix} \\ \vdots \\ \begin{bmatrix} x_{11g}, x_{12g}, \dots, x_{1(d-1)g} : y_{1g} \\ x_{21g}, x_{22g}, \dots, x_{2(d-1)g} : y_{2g} \\ \vdots \\ x_{r1g}, x_{r2g}, \dots, x_{r(d-1)g} : y_{rg} \end{bmatrix} \end{cases} \quad (1)$$

$$SM = \begin{bmatrix} sm_{11}, sm_{12}, \dots, sm_{1g} \\ sm_{21}, sm_{22}, \dots, sm_{2g} \\ \vdots \\ sm_{r1}, sm_{r2}, \dots, sm_{rg} \end{bmatrix} \quad (2)$$

where *x* represent inputs and *y* the output in a MISO system. *r* is a variable number of fuzzy rules, *d* is a constant number of input and output variables, and g is the variable number that represents the size of the discrete uncertainty dimension. *sm* represent weights for each rule and each uncertainty dimension.

The inference of an output follows the next steps:

1. Calculate the uncertainty rule-base *UNR* of dimension *r*-by-*d*; this is where the use of the secondary

membership lies. This calculation accounts for the type-reduction process:

$$UNR = \begin{bmatrix} unx_{11}, unx_{12}, \dots, unx_{1(d-1)} : uny_1 \\ unx_{21}, unx_{22}, \dots, unx_{2(d-1)} : uny_2 \\ \vdots \\ unx_{r1}, unx_{r2}, \dots, unx_{r(d-1)} : uny_r \end{bmatrix} \quad (3)$$

$$UNR_{ij} = \frac{\sum_{m=1}^{g} SM_{im} \cdot R_{ijm}}{\sum_{n=1}^{g} SM_{in}} \quad (4)$$

where *unx* represents uncertainty-weighted inputs and *uny* the uncertainty weighted output in a MISO system. For equation (4), $i=1,2,\dots,r$; and $j=1,2,\dots,d$.

2. Calculate the primary membership with the FCM algorithm and the *UNR* input reduced matrix:

$$UNRin = \begin{bmatrix} unx_{11}, unx_{12}, \dots, unx_{1(d-1)} \\ unx_{21}, unx_{22}, \dots, unx_{2(d-1)} \\ \vdots \\ unx_{r1}, unx_{r2}, \dots, unx_{r(d-1)} \end{bmatrix} \quad (5)$$

$$Dst_i = \sum_{n=1}^{d-1} (I_n - UNRin_{in})^2 \quad (6)$$

$$\mu_i = \sum_{l=1}^{r} \left(\frac{Dst_i}{Dst_l} \right)^{\frac{-1}{m-1}} \quad (7)$$

$$C_i = \frac{\mu_i - min\,(\mu_i)}{max\,(\mu_i) - min\,(\mu_i)} \quad (8)$$

where *UNRin* is the *UNR* input reduced matrix, $I(t) = [in_1, in_2, \dots, in_{(dim-1)}]$ is the input vector with the information needed to perform a prediction and is of size *1*-by-(*d*-1), Dst_i is the *1*-by-*r* distance vector, *m* is an FCM algorithm constant (i.e., usually equal to 2), μ_i is the *1*-by-*r* membership vector and *C* is the normalized *1*-by-*r* μ. $i=1,2,\dots,r$; and $n=1,2,\dots,(d\text{-}1)$. The FCM algorithm weights for each rule (see equation (7)), the sums of the squared distances between all *UNRin* elements and the current inputs (see equation (6)). This way, a normalized membership (see equation (8)) is computed for each rule.

3. Obtain the *PO* (predicted output) with the *UNR* output reduced vector. This corresponds to the defuzzification process;

$$UNRout = \begin{bmatrix} uny_1 \\ uny_2 \\ \vdots \\ uny_r \end{bmatrix} \quad (9)$$

This article has been accepted for publication in a future issue of this journal, but has not been fully edited. Content may change prior to final publication. Citation information: DOI 10.1109/TFUZZ.2016.2598363, IEEE Transactions on Fuzzy Systems

$$PO = \frac{\sum_{m=1}^{r} C_m \cdot UNRout_m}{\sum_{n=1}^{r} C_n} \quad (10)$$

where *UNRout* is the *UNR* output reduced matrix and *C* is the normalized *1*-by-*r* membership vector.

The A-GT2-FCM modelling algorithm is a GT2FL approach since it utilizes two membership sets in the computation of a predicted output. The secondary membership weights inside *SM* are used to calculate an uncertainty type-reduced rule-base *UNR* (step 1) that is later used to calculate the primary membership (step 2). This membership is computed with the FCM algorithm and compares each new input vector *I(t)* to all the rules in *UNR*. Predictions (step 3, equation (10)) are based on the comparison of the current state with the information stored in the tri-dimensional rule-base (*R* and *SM*). The modelling algorithm utilizes a very simplified inference by avoiding the costly Mamdani-type rule interpretation process. This way, it is able to take advantage of the uncertainty present in the data without the need of a computationally expensive type-reduction process that represents the bottleneck of many approaches to GT2FLS [42]. It is nevertheless a very powerful algorithm because of its learning and adaptive capability reinterpreted from the ideas of Gao [10] and Qi [9], where an automatically generated model through the use of similarity indexes is used for learning in real-time. Fig. 4 shows a diagram of the A-GT2-FCM modelling framework. A numerical example explaining further the A-GT2-FCM algorithm is presented in the Appendix section.

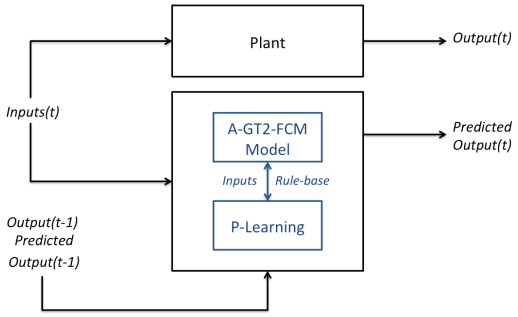

Fig. 4. Diagram of the Adaptive General Type-2 Fuzzy C-Means, A-GT2-FCM, modelling framework with its p-learning algorithm routine.

The learning algorithm in the A-GT2-FCM is named performance learning (p-learning) and is similar to the one in [9, 10] in its use of similarity measurements in the form of the inverse exponential function (see

This article has been accepted for publication in a future issue of this journal, but has not been fully edited. Content may change prior to final publication. Citation information: DOI 10.1109/TFUZZ.2016.2598363, IEEE Transactions on Fuzzy Systems

equations (11)-(13) and (15)). The p-learning algorithm includes the incorporation of similarity measurements to account for uncertainty and uses negative RL to weight this uncertainty. Additionally, rules are not replaced as in [9] but combined or added to uncertainty dimension with the aid of two similarity thresholds.

The p-learning algorithm operates with the following learning procedure:

1. After prediction (see equations (3) to (10)) acquire the actual output *O(t-1)* and check the maximum error tolerance *ET* (constant defined by the user) to decide if p-learning should be applied.

$$\text{If } E(t) = |PO(t-1) - O(t-1)| > ET,$$

apply p-learning (steps 2-13, equations (11) to (16))

2. In p-learning, calculate similarity index vector *RS* of size *1*-by-*(r-1)* (reinterpreted from [9]) among rules in uncertainty rule-base *UNR*. Use i=1,2,…,(*r-1*); j=1,2,…,d. This step identifies similar rules in the type-reduced rule-base (see equations (3) and (4)) using the constant *rad* (defined by the designer) as follows:

$$RS_i = e^{-\left(\sum_{j=1}^{d} \frac{\left|UNR_{ij} - UNR_{(i+1)j}\right|}{d \cdot rad}\right)} \tag{11}$$

3. Check *r* dimension combination threshold *CT* (constant defined by the designer and constrained by 1>*CT*>0). Obtain new *R* and *SM* using i=1,2,…,(*r*-1); j=1,2,…,d; k=1,2,…,g. If two or more rules are above the threshold, they are combined with λ_1 and λ_2 (constants defined by the designer).

$$\text{If } RS_i > CT, \text{ then}$$

$$R_{ijk} = \lambda_1 \cdot R_{ijk} + \lambda_2 \cdot R_{(i+1)jk}$$

$$SM_{ik} = \lambda_1 \cdot SM_{ik} + \lambda_2 \cdot SM_{(i+1)k}$$

$$\lambda_1 + \lambda_2 = 1$$

Erase $R_{(i+1)}$ for all d and g. Erase $SM_{(i+1)}$ for all g.

Reduce size of *r* by one

4. Calculate similarity index matrix *GS* of size *r*-by-*(g-1)* (reinterpreted from [9]) among rules in

This article has been accepted for publication in a future issue of this journal, but has not been fully edited. Content may change prior to final publication. Citation information: DOI 10.1109/TFUZZ.2016.2598363, IEEE Transactions on Fuzzy Systems

uncertainty dimension g with i=1,2,…,r; j=1,2,…,d; k=1,2,…,(g-1). With *rad*, defined similarly to step 2.

$$GS_{ik} = e^{-\left(\sum_{j=1}^{d} \frac{\left|g_{ijk} - g_{ij(k+1)}\right|}{d \cdot rad}\right)} \tag{12}$$

$$g_{ijk} = SM_{ik} \cdot R_{ijk}$$

5. Check g dimension generality threshold GT (constant defined by the designer with the constraint $1>CT>GT>0$) and obtain new R and SM with i=1,2,…,r; j=1,2,…,d; k=1,2,…,(g-1). If two or more uncertainty rule-mappings are similar, then they are combined as in step 3.

If $GS_{ik} > GT$,

$$R_{ijk} = \lambda_1 \cdot R_{ijk} + \lambda_2 \cdot R_{ij(k+1)};\ SM_{i(k+1)} = 0$$

Erase $R_{i(k+1)}$ for all d

6. Resize the rule-base by eliminating unnecessary dimensions after similarity checks of steps 3 and 5.

7. Calculate similarity index matrix DS of size r-by-d (reinterpreted from [9]) with past input-output vector $D(t-1) = [I(t-1), O(t-1)]$ of size 1-by-d, and rules in the rule-base. Use i=1,2,…,r; k=1,2,…,g with constant *rad* defined similarly to steps 2 and 4.

$$DS_{ik} = e^{-\left(\sum_{j=1}^{d} \frac{\left|D_j - R_{ijk}\right|}{d \cdot rad}\right)} \tag{13}$$

8. Check combination threshold CT to identify if new data is similar to an existing rule in the rule-base. If true, combine with existing rule and obtain new R and SM by combining D with the combination constant σ (chosen by de designer under the constraint $0<\sigma<1$). The combination constant σ expresses the degree of importance given to incoming new information. Use i=1,2,…,r; j=1,2,…,d; k=1,2,…,g.

If $DS_{ik} > CT$,

$$R_{ijk} = \sigma \cdot D_j + (1-\sigma) \cdot R_{ijk};\ SM_{ik} = \sigma + (1-\sigma) \cdot SM_{ik}$$

9. Check generality threshold GT. Add to uncertainty of one of the rules and obtain new R and SM. In case no similar rule is found in the rule-base, but D vector is similar enough as defined by the GT, add D to the uncertainty dimension g. Use i=1,2,…,r; j=1,2,…,d; k=1,2,…,g.

This article has been accepted for publication in a future issue of this journal, but has not been fully edited. Content may change prior to final publication. Citation information: DOI 10.1109/TFUZZ.2016.2598363, IEEE Transactions on Fuzzy Systems

Else if $DS_{ik}>GT$,

$$R_{ij(k+1)} = D_j; SM_{ij(k+1)} = 1$$

10. If the input-output mapping *D* is different to existing rules and their uncertainty dimension, add as a new rule for all *g* and obtain the new *R* and *SM*. This step generates new data rule-representatives for the rule-base. Use *i*=1,2,…,*r; j*=1,2,…,*d; k*=1.

Else,

$$R_{(r+1)j1} = D; SM_{(r+1)1} = 1$$

Increment size of *r* by one

11. Re-order rule-base sorting by output (*d*) column for interpretability of model.

12. Calculate the negative *RL* algorithm-based distance with the scaling constant α. Use *i*=1,2,…,*r; j*=1,2,…,*d; k*=1,2,…,*g*.

$$d_{ijk} = \left|\alpha(D_j - R_{ijk})\right| \tag{14}$$

If $\alpha = 1$, $d_{ijk} = \left|D_j - R_{ijk}\right|$

13. Calculate the RL based similarity matrix *RLS* of size *r*-by-*g* (reinterpreted from [9]). Use constant *rad* defined similarly to steps 2, 4 and 7. Obtain new *SM* matrix. In this step, equation (16) uses negative RL to reduce the weight of dissimilar representatives in dimension *g*. With this process and enough experienced data, the weights for less occurring cases stored in the uncertainty are reduced. This ensures that the predictions are more highly influenced by the most occurring cases when *SM* is used for the calculation of *UNR* (see equation (4)). Use *i*=1,2,…,*r; k*=1,2,…,*g*.

$$RLS_{ik} = e^{-\left(\sum_{j=1}^{d}\frac{d_{ijk}}{d\cdot rad}\right)} \tag{15}$$

$$SM_{ik} = \frac{SM_{ik}\cdot RLS_{ik}}{\max\left(RLS_i\right)} \tag{16}$$

As can be observed from the inference process and the p-learning process of the A-GT2-FCM modelling framework, the inter- and intra-parameter variabilities across humans in a HMI system are handled inside the model learning operation without the need for calibration processes.

This article has been accepted for publication in a future issue of this journal, but has not been fully edited. Content may change prior to final publication. Citation information: DOI 10.1109/TFUZZ.2016.2598363, IEEE Transactions on Fuzzy Systems

In addition to the modelling operation itself, the A-GT2-FCM framework can be re-utilised for control purposes given that it holds meaningful information about the dynamics of the system it is supervising. In the next section (V), a detailed account of one of the ways in which the inference process of the A-GT2-FCM can be re-utilised for control is addressed.

With regards to the modelling for the MA Operations Experiment of Section II, rule-base *R* was constructed with mappings of the psycho-physiological signal markers HRV_1, HRV_2, TLI_1, TLI_2 and PDM as inputs. The output was selected as *PAP* (predicted accuracy performance) for the MISO system. In this case *R* is of size *r*-by-*6*-by-*g*. *d=6* is constant while *r* and *g* may change their size according to the p-learning algorithm and the definition of the constants: m=2, $\lambda_1 = \lambda_2 = 0.5$, σ=0.2, *rad*=0.25, α=*1*, *ET*=0.05, *CT*=0.99 and *GT*=0.7. *SM* is of size *r*-by-*d*.

V. Energy Model-Based control

The inference process to produce a predicted output for A-GT2-FCM is supported by the FCM Membership calculation (equations (6)-(8)), obtained by comparing the input vector *I(t)* with the stored information about the relationships between inputs and output learned through the p-learning algorithm (equations (11)-(16)).

For the production of a control output, the inference process of A-GT2-FCM can be re-utilised with some simple modifications for its use as the Energy Model Based Controller (E-MBC). The model itself may not directly guide the system into the desired state accurately and because of this reason, an energy function, f_E, has instead been defined. The idea is to maximize 'energy' extraction by directing the system to states where 'maximum extraction of energy' is achieved. With the aid of this energy function, an additional energy membership vector *E* will be used in combination with the FCM membership *C* (that directs the inference into the most probable state given present conditions) for the production of a control output. Fig. 5 shows a diagram illustrating the E-MBC architecture.

The inference for the calculation of a control output can be explained as follows:

This article has been accepted for publication in a future issue of this journal, but has not been fully edited. Content may change prior to final publication. Citation information: DOI 10.1109/TFUZZ.2016.2598363, IEEE Transactions on Fuzzy Systems

1. Obtain an energy membership from the energy function f_E evaluated at each rule in the rule-base. The energy function f_E is defined by the designer to guide the controller towards the desired state and is an application specific function.

$$E_i = f_E\left(unx_{i1}, unx_{i2}, \dots, unx_{i(d-1)}, uny_i\right) \tag{17}$$

Where *E* is the energy membership vector of size *1*-by-*r*. *unx* and *uny* are uncertainty-weighted input and output elements from the uncertainty matrix *UNR* respectively; for a MISO system and *i*=1,2,…,*r*. The energy membership may use any combination of inputs and output as specified by the designer.

2. Use the energy membership in combination with the FCM membership of equation (8) for the calculation of a control output *CO*:

$$CO = \frac{\sum_{m=1}^{r}(\epsilon E_m + (1-\epsilon)C_m)\cdot UNRc_m}{\sum_{n=1}^{r}(\epsilon E_n + (1-\epsilon)C_n)} \tag{18}$$

where *UNRc* is the uncertainty-weighted control variable vector of size *r*-by-*1* from the uncertainty matrix *UNR*. *C* and *E* are the FCM and Energy memberships respectively (of size *1*-by-*r*). The constant ϵ is a user-selected weight. As a requirement, the control variable should be used as an input in the rule-base to ensure its relationship to other variables is stored and learned. The calculation of the *CO* action re-uses the inference process defined for the modelling framework.

For the control of the MA Operations Experiment (Section II), the control variable is represented by the Difficulty Level (*DL*) of the experiment. For this reason, this variable had to be added as another input for the model, with the mappings in *R* (e.g., of augmented size *r*-by-7-by-*g*) becoming (*i*=1,2,…,*r; k*=1,2,…,*g*):

$$R = [HRV_{1_{ik}}, HRV_{2_{ik}}, TLI_{1_{ik}}, TLI_{2_{ik}}, PDM_{ik}, DL_{ik} : PAP_{ik}] \tag{19}$$

For E-MBC to operate efficiently and optimally it is important that the rule-base (e.g., *R* and *SM*) explores and learns from the main operation regions of the system. For the MA experiment specifically, this translates to having experienced all the four difficulty levels. Fig. 6 shows the diagram of the E-MBC that was designed for the MA experiment. E-MBC for the MA experiment used the following inference steps:

This article has been accepted for publication in a future issue of this journal, but has not been fully edited. Content may change prior to final publication. Citation information: DOI 10.1109/TFUZZ.2016.2598363, IEEE Transactions on Fuzzy Systems

1. Use *DL* (e.g., one of the inputs to the model) as the control output.
2. Use the *PAP* (e.g., the output of the model) as an input for the E-MBC.
3. Calculate the *UNR* with equation (4) with *R* of equation (19) (i=1,2,…,r):

$$UNR = [unHRV_{1_i}, unHRV_{2_i}, unTLI_{1_i}, unTLI_{2_i}, unPDM_i, unPAP_i : unDL_i]$$

4. Define the energy function (see equation (17)) as dependent on the predicted accuracy performance and the difficulty level:

$$f_E(PAP, DL) = PAP \cdot DL/4$$

5. Calculate the energy membership and normalize it similarly to *C* in equation (8) (i=1,2,…,r):

$$\mu_{E_i} = \sum_{m=1}^{r} \frac{unPAP_i \cdot unDL_i}{unPAP_m \cdot unDL_m}$$

$$E_i = \frac{\mu_{E_i} - \min(\mu_{E_i})}{\max(\mu_{E_i}) - \min(\mu_{E_i})}$$

6. Calculate the FCM membership *C* following equations (6) to (8).
7. Calculate the controller output using equation (18) with $\epsilon = 0.5$.

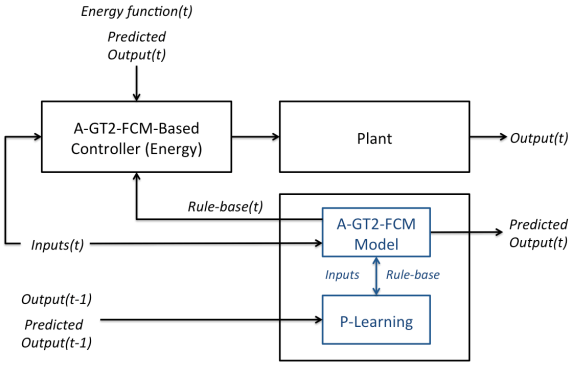

Fig. 5. Diagram of the Energy Model Based Controller, E-MBC, showing how it uses the information included in the A-GT2-FCM model.

The use of *PAP* and *DL* for guidance of the controller is driven by the fact that this control should maximize the difficulty level without compromising on accuracy. For every participant in the study, the ideal state (e.g., maximum *DL* without great loss in *AP*) will be influenced by his/her personal ability and

This article has been accepted for publication in a future issue of this journal, but has not been fully edited. Content may change prior to final publication. Citation information: DOI 10.1109/TFUZZ.2016.2598363, IEEE Transactions on Fuzzy Systems

current state identified through the psycho-physiological markers and *PAP* with his derived A-GT2-FCM model. Another important feature of E-MBC designed for the MA experiment is its use of a 1 min hysteresis that ensures that control actions have enough time to have a causal effect on the participant and to avoid 'bang-bang' control effect. Fig. 7 shows the normalized outcomes for the defined energy function $f_E(PAP, DL)$. From Fig. 7 it can be observed how the ideal state corresponds to *DL*=4 with an *AP=1*. As will be seen in the Results of Section VI, this difficulty level proved to be a challenge for all participants, with a lower *DL* being their ideal level of performance. It is worth noting that performance is greatly marked by the psycho-physiological state of the participant (e.g., influenced by fatigue, time of day, engagement, etc.); this is the part where the knowledge of the model output contributes most.

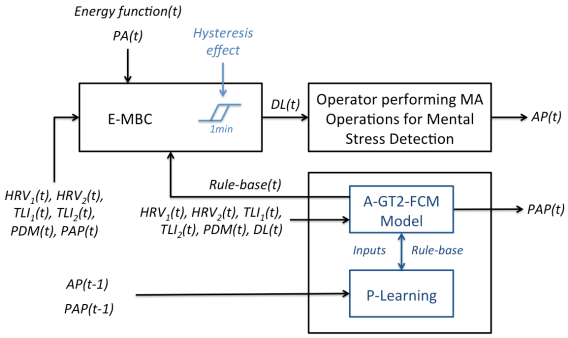

Fig. 6. Diagram of the Energy Model Based Controller designed for the MA experiment. The diagram shows how E-MBC uses the A-GT2-FCM model information stored in its rule-base and the inclusion of a 1 min hysteresis effect.

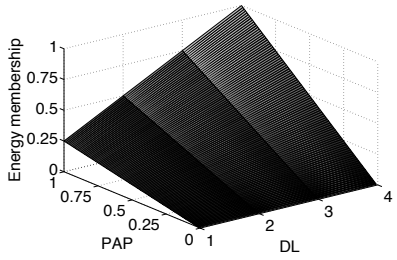

Fig. 7. Membership for the energy function $f_E(PAP, DL)$.

VI. RESULTS

This section outlines and discusses the results relating to modelling and control using the A-GT2-FCM framework of Section IV applied to the MA operations-based experiments of Section II. To highlight the

true adaptive/self-organising properties of this framework, it is compared with participant-specific ANFIS fixed models (i.e. one model per participant trained with data from ME-1) for off-line predictions with the same data obtained during the real-time A-GT2-FCM modelling experiments. Following these results and an analysis of the adaptive properties of the proposed framework, results concerning the real-time application of the E-MBC of Section V are described in more detail. Additionally, an ANFIS prediction-based reference controller (ANFIS-C) is tested with an additional set of experimental real-time sessions of comparable characteristics (i.e., same disturbance configuration, same experimental length, same participants). It is worth noting at this stage that a 'like for like' comparison between results with the two designed controllers is not always possible since variations in the real-time experiments are hard and even impossible to reproduce. However, the evidence presented in this section should still be helpful in evaluating the properties of the compared control systems.

The ANFIS participant-specific models were constructed with the MATLAB®-based 'Adaptive Neuro-Fuzzy Modeling GUI'. The models were trained with real data from ME-1 and validated with real data from ME-2. The ANFIS structure was derived using subtractive clustering for each participant, leading to rule-bases of 10 to 12 fuzzy TSK-based rules. The inputs for the ANFIS model were $I_{ANFIS} = [HRV_1(t),\ HRV_2(t), TLI_1(t), TLI_2(t), PDM(t), AP(t-1)]$. The output is the same as for the A-GT2-FCM modelling framework, i.e. *PAP(t)*. The ANFIS model parameters were trained with the hybrid off-line learning algorithm available in the MATLAB® Fuzzy Logic Toolbox™ .

A. Modelling results

As described in Section II one experimental session with two real-time modelling experiments was performed for every participant in the study. The first experiment consisted of an incremental difficulty configuration while the second consisted of a scrambled difficulty configuration as illustrated in Fig. 3.

For the first prediction to be obtained from A-GT2-FCM, an initial 'dummy' rule was included which ensured that the first prediction was of an accuracy of 1. Afterwards, the p-learning algorithm took over and elicited new meaningful fuzzy rules based on the psycho-physiological markers and the observed past

This article has been accepted for publication in a future issue of this journal, but has not been fully edited. Content may change prior to final publication. Citation information: DOI 10.1109/TFUZZ.2016.2598363, IEEE Transactions on Fuzzy Systems

model output.

In order to evaluate the performance of A-GT2-FCM and to compare it with the participant-specific ANFIS model results, a table was constructed to show the errors and correlations of predictions; these indices were calculated using equations (20) and (21) respectively:

$$Error = 100 \cdot \sqrt{\frac{\sum_{i=1}^{N}(AP_i - PAP_i)^2}{N}} \tag{20}$$

$$Correlation = \frac{\mathrm{cov}(AP,PAP)}{\sqrt{\mathrm{cov}(AP,AP)\cdot\mathrm{cov}(PAP,PAP)}} \tag{21}$$

where N is the total number of samples in the experiment. For all experiments $N=690$, that corresponds to 150 samples (samples are calculated with data from 30 s shifted every 1 s) for Phase 1 and 180 samples for Phases 2 through 4 each.

Table I presents the modelling results (calculated via equations (20) and (21)) for the predictions in real-time which were obtained via A-GT2-FCM and compared with the off-line predictions with the same experimental data of the participant-specific ANFIS models. From Table I it can be observed that A-GT2-FCM performs better and in a consistent way for all participants in the study. Errors and Correlations show an excellent performance throughout, demonstrating the fast learning capabilities of the algorithm that needs no training phase. In the case of ANFIS, a very small training error and a high correlation index are observed for every participant in ME-1. However, the performance for ME-2 is not consistent and shows inferior prediction results for most participants. Overall A-GT2-FCM is able to obtain superior predictions; which can mainly be attributed to its adaptive properties. To further demonstrate the ability of A-GT2-FCM, Figs. 8 through 11 show the results for ME-1 and ME-2 for P01 together with the markers acquired for these experiments.

From Figs. 9 and 11 it can be observed how A-GT2-FCM was able to successfully predict the performance of P01 in the MA experiment for both ‘difficulty’ configurations (ME-1 and ME-2). Furthermore, correlation, as shown in Table I, is very high and the error is very small. The information used by A-GT2-FCM to calculate its predictions is presented in Figs. 8 and 10 and corresponds to the

This article has been accepted for publication in a future issue of this journal, but has not been fully edited. Content may change prior to final publication. Citation information: DOI 10.1109/TFUZZ.2016.2598363, IEEE Transactions on Fuzzy Systems

studied psycho-physiological markers of Section II. Similar performances were obtained for all participants in the study despite the intra-differences between them. For ANFIS, the inputs correspond to the same markers of Figs. 8 and 10 but with the inclusion of $AP(t\text{-}1)$. Fig. 10 also shows the predictions for P01-specific ANFIS model in the case of ME-2, demonstrating the inability of ANFIS fixed model to handle the inter-parameter differences in P01. However, from Table I it can be observed how some of the ANFIS models were also able to obtain good predictions. Even in these cases, the inability of a fixed model to handle such parameter variations is apparent.

TABLE I

A-GT2-FCM real-time / ANFIS off-line, Modelling

Error

	ME-1	ME-2
P01	5.4197 / 2.0520	6.1525 / 71.8948
P02	5.2753 / 2.2577	6.7112 / 52.0001
P03	5.7502 / 1.8520	6.2016 / 34.0385
P06	8.1281 / 3.1923	6.7512 / 58.8248
P07	6.4311 / 2.5943	6.9501 / 43.7482
P08 *	4.7957 / 1.7297	5.1479 / 6.9308
P09	5.1887 / 1.4180	5.2014 / 8.2639
P10	5.1957 / 1.9126	6.4262 / 9.4716
P11	5.0032 / 2.3427	5.8235 / 6.4813
P12	6.4129 / 2.2724	6.7505 / 14.3965
Avg	5.7601 / **2.1624**	**6.2116** / 30.6051

Correlation

	ME-1	ME-2
P01	0.9828 / 0.9971	0.9587 / 0.1716
P02	0.9820 / 0.9966	0.9732 / 0.4876
P03	0.9638 / 0.9833	0.9574 / 0.6257
P06	0.9751 / 0.9955	0.9818 / 0.3718
P07	0.9866 / 0.9976	0.9826 / 0.3332
P08 *	0.9852 / 0.9977	0.9682 / 0.9601
P09	0.9662 / 0.9972	0.9553 / 0.9073
P10	0.9818 / 0.9970	0.9860 / 0.9662
P11	0.9859 / 0.9968	0.9856 / 0.9834
P12	0.9845 / 0.9975	0.9814 / 0.9216
Avg	0.9794 / **0.9956**	**0.9730** / 0.6729

*** Both experiments with incremental difficulty**

It is worth noting that the psycho-physiological markers used were re-scaled (HRV_1/2500, HRV_2/1.2, TLI_1/120, TLI_2/200 PDM/30) with constant values for all ten participants; this was a requirement for the programed software. However, this modelling framework does not necessarily require any type of normalization procedure for it to operate successfully.

B. Adaptive properties of the A-GT2-FCM Modelling Framework

In this section the adaptive properties of A-GT2-FCM are addressed. It was stated in Section IV that the algorithm presents characteristics that make it adaptable to inter- and intra-parameter variabilities between

This article has been accepted for publication in a future issue of this journal, but has not been fully edited. Content may change prior to final publication. Citation information: DOI 10.1109/TFUZZ.2016.2598363, IEEE Transactions on Fuzzy Systems

the participants in the study given its ability to handle uncertainty from its GT2FL configuration and its real-time p-learning negative RL algorithm. The evidence that supports these adaptive characteristics is discussed in the points below:

1 The model is able to operate and self-organize in real-time. From the real-time modelling results presented in Table I and Figs. 9 and 10 it is evident that A-GT2-FLS is capable of learning from features in the data and in real-time and of producing good predictions even without a training phase. Further, and on the subject of the self-organization properties of the modelling framework, Fig. 12 illustrates how the p-learning algorithm operates by displaying the number of rules in r and g dimensions as DL changes for P12 in ME-1. The P12-specific ANFIS model is of similar rule-base size with 12 rules leading to good off-line predictions for the training ME-1 data.

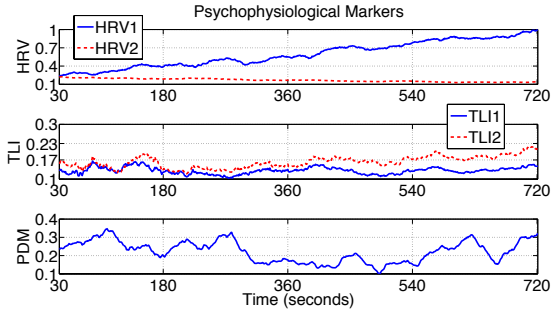

Fig. 8. P01 Psycho-physiological markers inputs (HRV1, HRV2, TLI1, TLI2 and PDM) to A-GT2-FCM. Incremental difficulty (ME-1 with DL= 1, 2, 3, 4) MA experiment.

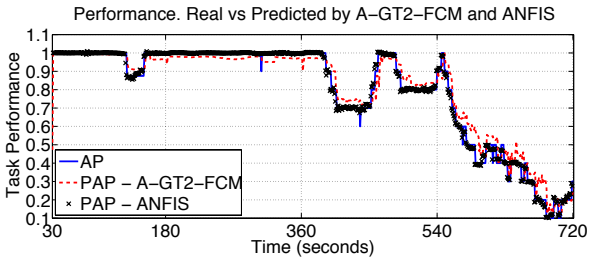

Fig. 9. P01 Accuracy performance, AP, predicted accuracy performance, PAP for A-GT2-FCM in real-time and off-line with P01-specific ANFIS model. Incremental difficulty (ME-1 with DL= 1, 2, 3, 4) MA experiment.

This article has been accepted for publication in a future issue of this journal, but has not been fully edited. Content may change prior to final publication. Citation information: DOI 10.1109/TFUZZ.2016.2598363, IEEE Transactions on Fuzzy Systems

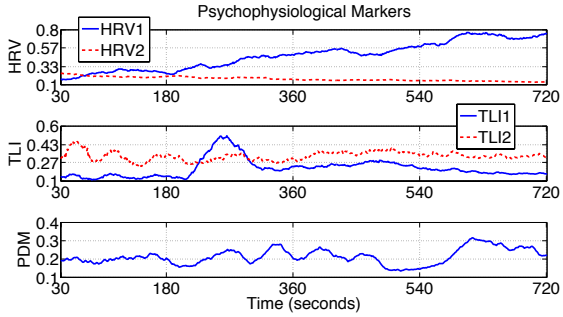

Fig. 10. P01 Psycho-physiological markers inputs (HRV1, HRV2, TLI1, TLI2 and PDM) to A-GT2-FCM. Scrambled difficulty (ME-2 with DL= 2, 3, 1, 4) MA experiment.

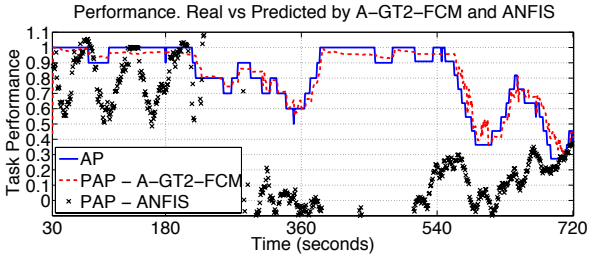

Fig. 11. P01 Accuracy performance, AP, predicted accuracy performance, PAP for A-GT2-FCM in real-time and off-line with P01-specific ANFIS model. Scrambled difficulty (ME-2 with DL= 2, 3, 1, 4) MA experiment.

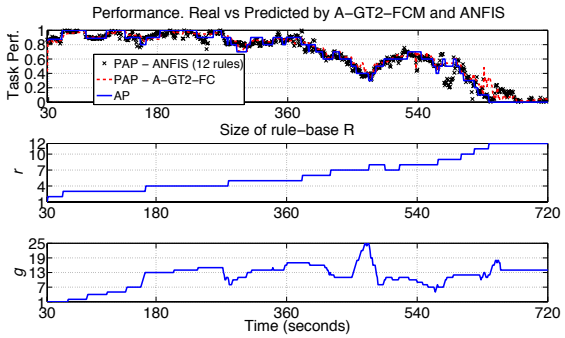

Fig. 12. Evolution in the size of the rule-base R during ME-1 for P12. Top plot, Task Performance (A-GT2-FCM and P12-based ANFIS).

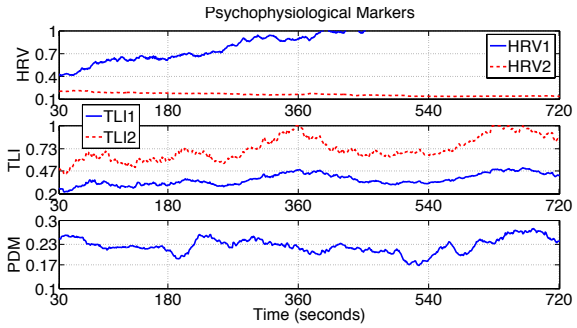

Fig. 13. Psycho-physiological markers input (HRV1, HRV2, TLI1, TLI2 and PDM) for the ME-2 with DL= 2, 3, 1, 4. MA operations experiment for P11.

2 The modelling framework is generalizing for all participants; there was no need for a participant-based calibration and off-line model construction, an important contribution when compared with the ANFIS case and the works in [3, 16]. The same 'dummy' first prediction rule-base was used for all participants. Additionally, despite having variability in the psycho-physiological inputs from participant to participant and among participants themselves, the model was able to capture these variabilities in a transparent way. In fact, the same constant values were used to scale the markers for all participants. In order to further demonstrate these facts, input markers for ME-2 (scrambled difficulty) for P11 are displayed in Fig. 13. From this figure it can be observed that the numerical values for the markers of P11 differ significantly from the ones presented for P01 in Fig. 10 (see y-axis). This is especially evident for the TLI markers, since for P11 these are double in magnitude when compared to the ones from P01 for the same experimental configuration. Inter-differences in marker scaling are also evident when further examining the TLI markers for P01 in Figs. 8 and 10. In this particular case, the markers for ME-2 (Fig. 10) are double in magnitude when compared with the markers of ME-1 (Fig. 8). This important change in marker scaling is probably responsible for the degraded predictions observed for the P01-specific ANFIS model in ME-2 (see Fig. 11).

3 A-GT2-FCM can handle and adapt to temporal loss of information. Given the conditions for real-time acquisition and calculation of markers, there were occasional losses of information resulting from reference disconnections on the head scalp during EEG acquisition for some experiments. However, A-GT2-FCM was able to adapt to these disturbances without any significant loss in performance; Figs. 14 and 15 represent one of such cases. Fig. 14 includes a scenario whereby the EEG-based TLI markers are lost during phase 3 of ME-2 for P02. The effect of this can also be observed in Fig. 15 at the same time-stamps (with evident lower than average predictions for the location) for the loss and the recovery of A-GT2-FCM (see circled regions in Figs. 14 and 15). In these graphs, the ability of the adaptive model to recover quickly at the next iteration is also apparent, ensuring successful adaptation and disturbance rejection. For ANFIS, the situation appears to be rather different, leading to a poor performance for ME-2

This article has been accepted for publication in a future issue of this journal, but has not been fully edited. Content may change prior to final publication. Citation information: DOI 10.1109/TFUZZ.2016.2598363, IEEE Transactions on Fuzzy Systems

with no robustness properties for intra-parameter changes in P02 and for temporal loss of marker information.

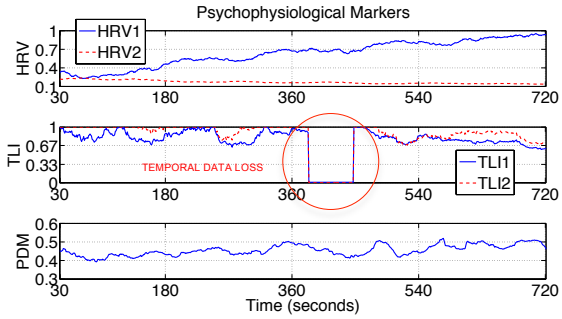

Fig. 14. Psycho-physiological markers input (HRV1, HRV2, TLI1, TLI2 and PDM) for the ME-2 with DL= 2, 3, 1, 4. MA operations experiment for P02. Loss of data during phase 3 for EEG based markers.

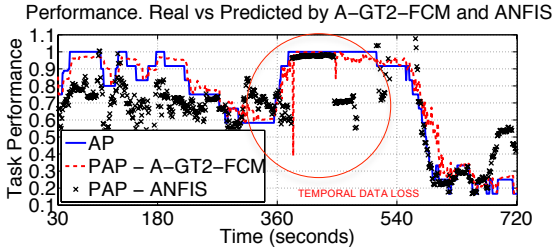

Fig. 15. Accuracy performance and predicted accuracy performance obtained with A-GT2-FCM in real-time and off-line with the P02-specific ANFIS model. Scrambled difficulty ME-2 with DL= 2, 3, 1, 4 for P02. Loss of data during phase 3 for EEG based markers.

C. Energy Model-Based Control and ANFIS Prediction-Based Reference Control

This section discusses the results of the application of E-MBC and its comparison with the ANFIS prediction-based reference controller (ANFIS-C) using the same 10 participants from the real-time modelling experiments. As was previously explained, for the E-MBC to provide meaningful control actions it requires to have previously experienced the main system states.

Fig. 16 displays the model surfaces used for P12 E-MBC real-time experiment (top row plots) and the surfaces for P12-specific ANFIS model (bottom row plots). This figure shows how ANFIS tries to extrapolate behaviour (unsuccessfully) in some input spaces of the marker values; this is not the case for A-GT2-FCM.

This article has been accepted for publication in a future issue of this journal, but has not been fully edited. Content may change prior to final publication. Citation information: DOI 10.1109/TFUZZ.2016.2598363, IEEE Transactions on Fuzzy Systems

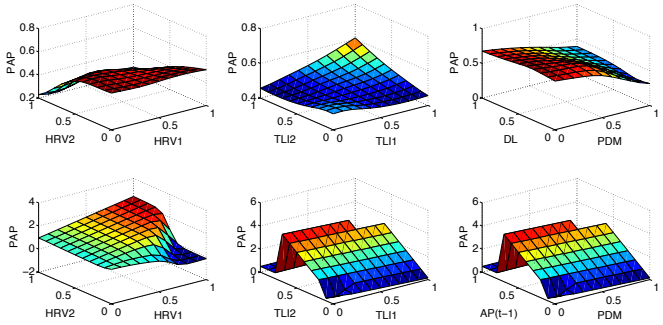

Fig. 16. Plant model for P12 after an off-line training with data gathered in real-time. Top surfaces, A-GT2-FCM as was used for the E-MBC experiment. Bottom surfaces, P12-specific ANFIS model with unsuccessful extrapolations.

The ANFIS-C design was based on the work of [22], where predictions from a fuzzy modelling framework were used together with a reference-based control approach. The ANFIS-C is based on the same reference configuration as above and uses the last minute averaged predicted performance to select the DL as the control output. The ANFIS-C is governed by the following steps [22]:

1. Obtain mean of last minute of PAP by participant-specific ANFIS model.
2. If *PAP>0.9*, then *DL=DL+1*; with maximum *DL=4*
3. Else if *PAP<0.6*, then *DL=DL-1*; with minimum *DL=1*
4. Else, *DL* remains unchanged.

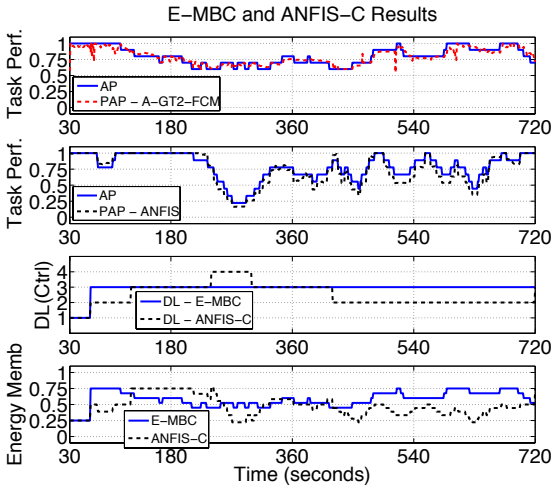

Fig. 17. E-MBC (mean energy extraction = 0.5809) and ANFIS-C (mean energy extraction = 0.4722) experiments in real-time for P11.

This article has been accepted for publication in a future issue of this journal, but has not been fully edited. Content may change prior to final publication. Citation information: DOI 10.1109/TFUZZ.2016.2598363, IEEE Transactions on Fuzzy Systems

Fig. 17 shows the results for the real-time E-MBC and ANFIS-C experiments performed for P11 in the study. From Fig. 17 it can be observed that after one minute of operation E-MBC selected *DL=3* from an initial *DL=1* as the best combination of *PAP* and the highest *DL*. After the selection of this *DL* there was an increase in the energy extraction that was maintained throughout the experiment. In contrast, despite having acceptable predictions, ANFIS-C increases the control DL in the second stage (*t=180s* to *t=360s*), which leads to a significant reduction in the task performance. It is worth noting that accurate performance predictions and model interpretability (e.g., the energy membership) at each operation stage are crucial in order to avoid reductions in accuracy and to maximize energy extraction. In this respect the ANFIS-C is deficient since it is only based on performance and does not consider the ideal *PAP- DL* combination (i.e., the energy membership) for each participant.

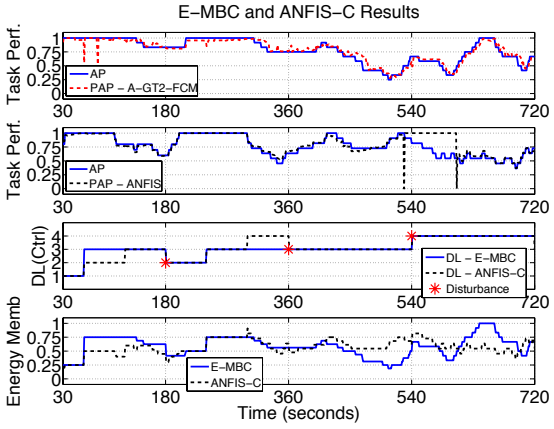

Fig. 18. E-MBC and ANFIS-C experiments in real-time for P08. Disturbances identified with an asterisk.

To further illustrate E-MBC's capabilities additional experiments were performed with disturbances (represented by a finite number of forced changes in DL) introduced at time stamps *t={180, 360, 540}*. Fig. 18 illustrates one of these experiments for P08 in the study; with disturbances identified with an asterisk. In this figure E-MBC identified that the best performance was achieved at *DL=3* (similarly to Fig. 17 for P11) by interpreting P08 ability from the information stored in its rule-base. From previous experience, E-MBC avoids *DL=4* during most of the experiment. However, after the disturbance a *t =540* the E-MBC adapted

This article has been accepted for publication in a future issue of this journal, but has not been fully edited. Content may change prior to final publication. Citation information: DOI 10.1109/TFUZZ.2016.2598363, IEEE Transactions on Fuzzy Systems

by leaving the *DL=4* unchanged given new experience of increased ability from P08. The ANFIS-C is only based on *PAP* and because of this reason, selected *DL=4* at stage 2 which reduces the *AP* greatly. During stage 4, bad predictions lead to ANFIS-C maintaining *DL=4* throughout the rest of this phase, leading to reduced energy extraction as can be identified in the bottom plot.

Fig. 19 shows another example for E-MBC operation for P12 where the way the size of the rule-base changes is also illustrated. It is worth noting that the size of g increases with the appearance of disturbances, which was expected since this dimension is linked to uncertainty. An experiment with the same structure and for the same participant was performed using ANFIS-C and is shown in Fig. 20. Under this controller P12 accuracy performance showed noticeable degradation following 'sub-optimal' model predictions.

In order to further evidence the increase in the energy extraction from the application of E-MBC, Table II includes the means of selected examples that compare the real energy extraction (mean($AP \cdot DL/4$)) of similar experiments with E-MBC, ANFIS-C and no control (open-loop). This comparative study is considered to be 'fair' since the introduced disturbances coincide with the *DL* profiles for the modelling experiments of Fig. 3. E-MBC and ANFIS-C take actions over these *DL* profiles in order to obtain an improved performance.

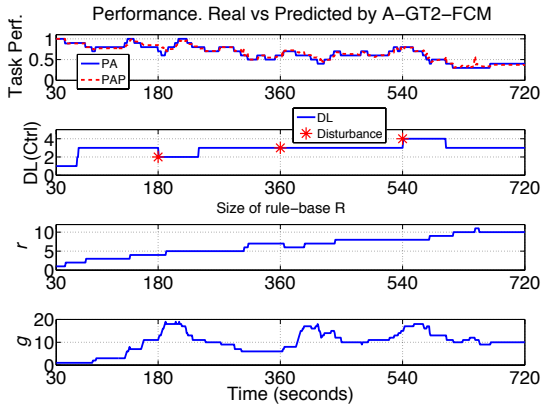

Fig. 19. Evolution of the size of the rule-base R during the E-MBC experiment for P12.

This article has been accepted for publication in a future issue of this journal, but has not been fully edited. Content may change prior to final publication. Citation information: DOI 10.1109/TFUZZ.2016.2598363, IEEE Transactions on Fuzzy Systems

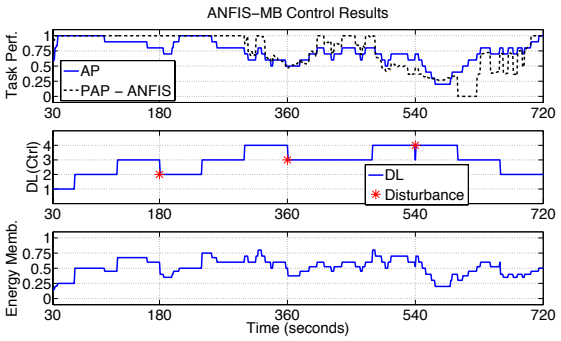

Fig. 20. ANFIS-C experiment in real-time for P12

As can be observed from Table II and for all participants with the exception of P02, E-MBC leads to an improvement in the amount of energy extracted when compared with the energy extraction without control. When compared with ANFIS-C, E-MBC shows better energy extraction in most cases. Overall, and for these 8 cases, there is an increase in energy performance as can be observed in the average values at the bottom of the Table. Furthermore, Fig. 21 shows the energy extraction results for P03 in the study with and without control. From this figure it can be observed that during the experiment, the real energy membership was mostly higher in the case of E-MBC. This is also evident from Table II for the mean energy extraction values for P03. This demonstrates how control actions derived from accurate predictions and model interpretability result in an increase in energy extraction.

TABLE II

Control Energy Extraction Mean			
	ANFIS - Ctrl	***E-MB Ctrl***	***No Control***
Experiment 1 (Incremental Difficulty)			
P01	0.5558	0.5699	0.4568
P07	0.4048	0.4247	0.2811
P08	0.5730	0.5848	0.4681
P12	0.5146	0.4614	0.3500
Experiment 2 (Scrambled Difficulty)			
P02	0.4049	0.3722	0.4046
P03	0.4760	0.5706	0.4104
P06	0.4163	0.4020	0.3340
P09	0.5286	0.6402	0.4969
Avg	**0.4843**	**0.5032**	**0.4002**

This article has been accepted for publication in a future issue of this journal, but has not been fully edited. Content may change prior to final publication. Citation information: DOI 10.1109/TFUZZ.2016.2598363, IEEE Transactions on Fuzzy Systems

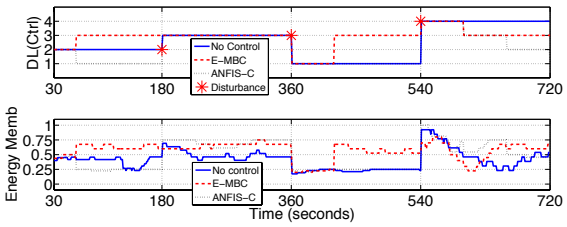

Fig. 21. Energy extraction results in real-time for P03 with and without controllers. Difficulty level profiles (top plot) and real energy membership (bottom plot).

VII. Conclusion

The starting point of this study was an experimental design based on Mental Arithmetic operations, which was selected to produce mental stress on a Human Machine Interaction configuration for 10 participants. The paper stressed that the MA experiment was capable of producing 'stress entrainment' of participants as evidenced by previously published literature applications using similar experimental configurations.

Furthermore, this experiment is simple and can be replicated for validation with no training required of participants. A Graphical-User-Interface-based software was also designed for the deployment of the experiment. This system handled all processes in the experiment that ranged from the acquisition of key psycho-physiological markers, to signal processing aspects, to modelling and real-time control calculations.

In terms of the psycho-physiological markers used to assess the participant's mental stress, HRV and TLI were identified as viable. Additionally, this paper introduced the use of a relatively new marker based on measurements of the pupil size, which according to surveyed literature, correlates strongly with performance breakdown in humans.

Using these design features, a new modelling technique named Adaptive General Type-2 Fuzzy C-Means was proposed and applied to modelling humans undergoing psychological (mental) stress. This new modelling technique was compared with participant-specific trained ANFIS models, and was shown to lead to superior predictions for checking data for all participants. The design of A-GT2-FCM technique incorporates features that make it adaptive to inter- and intra- parameter variability across subjects. This capability arises from its performance-learning algorithm based on negative Reinforcement Learning. This

learning algorithm proved its ability in the extraction of features from data in real-time, taking advantage of the capability of Fuzzy Type-2 sets to truly handle uncertainty. For all 10 participants in the study, modelling was achieved with a small error and a high correlation with the actual performance.

A controller design that re-exploits the A-GT2-FCM inference mechanism and information in the form of its fuzzy rule-base was also presented. This controller, named Energy Model Based Control (E-MBC) incorporates an Energy-based membership that allows it to acquire maximum energy extraction. Evidence to the controller's good performance was presented and compared with another set of real-time experiments of the same structure performed with a participant-specific ANFIS prediction-based reference control. E-MBC achieved superior performance with an overall 10% increase in the extraction of 'energy' for experiments without control. This comparative study and previous studies (e.g. [16]) highlighted the importance of using adaptive models and self-organising control for such harsh environment characterized by uncertainty and subject parameter variability.

The results achieved in this study show true promise in the further evaluation of the A-GT2-FCM modelling framework for applications with similar characteristics in the field of HMI. Furthermore, the simplicity of the inference mechanism designed for this algorithm makes it truly open to new and exciting control configurations for the many other challenging real-world environments where man-machine synergies and the switching between manual control and automation in real-time to avoid operator breakdown are of paramount importance.

APPENDIX

A numerical example detailing the A-GT2-FCM inference process of Section IV.

An example of a simple rule-base with r=d=g=3 is as follows:

$$R_{ex} = \left\{ \begin{bmatrix} 0.91\,,\,0.22\colon 0.52 \\ 0.76\,,\,0.39\colon 0.77 \\ 0.80\,,\,0.36\colon 0.90 \end{bmatrix}_1 \begin{bmatrix} 0.95\,,\,0.18\colon 0.59 \\ 1.00\,,\,0.79\colon 1.00 \\ -\,,\,-\colon - \end{bmatrix}_2 \begin{bmatrix} 0.86\,,\,0.21\colon 0.37 \\ -\,,\,-\colon - \\ -\,,\,-\colon - \end{bmatrix}_3 \right.,$$

This article has been accepted for publication in a future issue of this journal, but has not been fully edited. Content may change prior to final publication. Citation information: DOI 10.1109/TFUZZ.2016.2598363, IEEE Transactions on Fuzzy Systems

$$SM_{ex} = \begin{bmatrix} 0.75\,,\,0.32\colon 1.00 \\ 0.35\,,\,0.00\colon 0.00 \\ 1.00\,,\,-\colon - \end{bmatrix}$$

To calculate UNR_{ex} with equation (4) consider the following calculation of one of its output elements:

$$uny_1 = (sm_{11} \cdot y_{11} + sm_{12} \cdot y_{12} + sm_{13} \cdot y_{13})/(sm_{11} + sm_{12} + sm_{13})$$

$$= (0.75 \cdot 0.52 + 0.32 \cdot 0.59 + 1 \cdot 0.37)/(0.75 + 0.32 + 1) = 0.46$$

Similarly, all UNR_{ex} elements were obtained:

$$UNR_{ex} = \begin{bmatrix} 0.89\,,\,0.21\,,\,0.46 \\ 0.76\,,\,0.39\,,\,0.77 \\ 0.80\,,\,0.36\,,\,0.90 \end{bmatrix}$$

Consider an input vector:

$$I_{ex} = [0.66\,,\,0.27] \text{ with } UNRin_{ex} = \begin{bmatrix} 0.89\,,\,0.21 \\ 0.76\,,\,0.39 \\ 0.80\,,\,0.36 \end{bmatrix}$$

then, the first element of the distance vector in equation (6) is:

$$Dst_1 = (in_1 - unx_{11})^2 + (in_2 - unx_{12})^2 = (0.66 - 0.89)^2 + (0.27 - 0.21)^2 = 0.0576$$

With similar calculations, $Dst_2 = 0.0244$ and $Dst_3 = 0.0277$. The FCM membership (equation (7)) for the first rule can be calculated with *m=2* as follows:

$$\mu_1 = Dst_1^{\frac{-1}{m-1}} \Big/ \left(Dst_1^{\frac{-1}{m-1}} + Dst_2^{\frac{-1}{m-1}} + Dst_3^{\frac{-1}{m-1}} \right)$$

$$= (0.0576)^{-1}/[(0.0576)^{-1} + (0.0244)^{-1} + (0.0277)^{-1}] = 0.1838$$

Similarly, $\mu_2 = 0.4339$ and $\mu_3 = 0.3822$; and $C_1 = 0$, $C_2 = 1$, $C_3 = 0.7932$ after the normalization process in equation (8). With:

$$C_{ex} = [0\,,\,1\,,\,0.7932] \text{ and } UNRout_{ex} = [0.46\,,\,0.77\,,\,0.90]^T$$

the inference output of equation (10) is as follows:

$$PO_{ex} = \frac{C_1 \cdot uny_1 + C_2 \cdot uny_2 + C_3 \cdot uny_3}{C_1 + C_2 + C_3} = \frac{(0)(0.46) + (1)(0.77) + (0.7932)(0.90)}{0 + 1 + 0.7932} = 0.8275$$

REFERENCES

[1] L. A. Torres-Salomao, M. Mahfouf and E. El-Samahy, "Pupil Diameter Size Marker for Incremental Mental Stress Detection" in *2015 IEEE 17th International Conference on e-Health Networking, Applications and Services*, Boston, MA, 2015, pp. 14-17.

[2] C. E. Billings, *Aviation Automation: The Search for a Human-Centered Approach*. Mahwah:Lawrence Erlbaum Associates, 1996.

[3] L. A. Torres-Salomao, M. Mahfouf and O. Obajemu, "Interval Type-2 Fuzzy Logic Adaptive Modelling for Human Operators Undergoing Mental Stress", in *Proceedings of 19th World Congress of the International Federation of Automatic Control*, Cape Town, 2014, pp. 9880-9885.

[4] P. A. Hancock, "On the process of automation transition in multitask human–machine systems", *IEEE Transactions on Systems, Man and Cybernetics, Part A: Systems and Humans*, vol. 37, no. 4, pp. 586–598, 2007.

[5] N. Meshkati, "Control rooms' design in industrial facilities", *Human Factors and Ergonomics in Manufacturing Journal*, vol. 13, no. 4, pp. 269-277, 2003.

[6] P. A. Hancock and P. A. Desmond, *Stress, Workload, and Fatigue*. Mahwah:Lawrence Erlbaum Associates, 2001.

[7] C.-F. Juang and C.-Y. Chen, "Data-Driven Interval Type-2 Neural Fuzzy System With High Learning Accuracy and Improved Model Interpretability", *IEEE Transactions on Cybernetics*, vol. 43, no. 6, pp. 1781-1795, Dec. 2013.

[8] C.-F. Juang and C.-D. Hsieh, "A Fuzzy System Constructed by Rule Generation and Iterative Linear SVR for Antecedent and Consequent Parameter Optimization", *IEEE Transactions on Fuzzy Systems*, vol. 20, no. 2, pp. 372-384, April 2012.

[9] R. Qi and M. A. Brdys, "Adaptive Fuzzy Modelling and Control for Discrete-Time Nonlinear Uncertain Systems", in *2005 American Control Conference*, 2005.

[10]Y. Gao and M. J. Er., "Online adaptive fuzzy neural identification and control of a class of MIMO nonlinear systems", *IEEE Transactions on Fuzzy Systems*, vol. 11 no. 4, pp. 462-477, Aug. 2003.

[11]C. Hwang and F. C.-H. Rhee, "Uncertain Fuzzy Clustering: Interval Type-2 Fuzzy Approach to C-Means", *IEEE Transactions on Fuzzy Systems*, vol. 15, no. 1, pp. 107-120, Feb. 2007.

[12]A. Bagherjeiran, C. F. Eick and R. Vialta, "Adaptive Clustering: Better Representatives with Reinforcement Learning". Department of Computer Science, University of Houston, Houston, USA, March 2005.

[13]M. Delgado, A. F. Gómez-Skarmeta and F. Martin, "A fuzzy clustering-based rapid prototyping for fuzzy rule-based modeling", *IEEE Transactions on Fuzzy Systems*, vol. 5, no. 2, pp. 223-233, May 1997.

[14]J.-H Lin and C. Isik, "Fuzzy modeling and control based on maximum entropy self-organizing nets and cell state mapping", in *1997 Annual Meeting of the North American Fuzzy Information Processing Society*, 1997, pp. 45-50.

[15]O. Uncu and I. B. Turksen, "Discrete Interval Type 2 Fuzzy System Models Using Uncertainty in Learning Parameters", *IEEE Transactions on Fuzzy Systems*, vol. 15, no. 1, pp. 90-106, Feb. 2007.

[16]C. H. Ting, M. Mahfouf, A. Nassef, D. A. Linkens, G. Panoutsos, P. Nickel, A. C. Roberts and G. R. J. Hockey, "Real-Time Adaptive Automation System Based on Identification of Operator Functional State in Simulated Process Control Operations", *IEEE Transactions on Systems, Man and Cybernetics*, vol. 40, no. 2, pp. 251-262, 2010.

[17]A. H. Garde, B. Laursen, A. H. Jorgensen and B. R. Jensen, "Effects of mental and physical demands on heart rate variability during computer work", *European Journal of Applied Phisiology*, vol. 87, pp. 456-461, 2002.

[18]N. Hjortskov, D. Rissén, A. K. Blangsted, N. Fallentin, U. Lundberg and K. Sogaard, "The effect of mental stress on heart rate variability an blood pressure during computer work", *European Journal of Applied Physiology*, vol. 92, pp. 84-89, 2003.

[19]E. S. Mezzacappa, R. M. Kelsey, E. S. Katkin and R. P. Sloan, "Vagal Rebound and Recovery From Psychological Stress", *Psychosomatic Medicine*, vol. 63, pp. 650-657, 2001.

[20]L. Bernardi, J. WdowczykSzulc, C. Valenti, S. Castoldi, C. Passino. G. Spadacini and P. Sleight, "Effects of Controlled Breathing, Mental Activity and Mental Stress With or Without Verbalization on Heart Rate Variability", *Journal of the American College of Cardiology*, vol. 35, no. 6, pp. 1462-1469, 2000.

[21]A. Vincent, I. M. Craik, and J. J. Furedy, "Relations among memory performance, mental workload and cardiovascular responses", *International Journal of Psychophysiology*, vol. 23, pp. 181-198, 1996.

[22]E. Elsamahy, M. Mahfouf, L. A. Torres-Salomao and J. Anzurez-Marin, "A New Computer Control System for Mental Stress Management using Fuzzy Logic", in *2015 IEEE Conference on Evolving and Adaptive Intelligent Systems,* Douai, Dec. 2015.

[23]J.-S. R. Jang, "ANFIS: adaptive-network-based fuzzy inference system", *IEEE Transactions on Systems, Man and Cybernetics*, vol. 23, no. 3, pp. 665-685, May/Jun 1993.

[24]R. M. Stern, W. J. Ray and K. S. Quigley, *Psychophysiological Recording*, New York:Oxford University Press, 2001.

[25]S. Akselrod, D. Gordon, F. A. Uvel, D. Shannon, C. A. Barger and R. J. Cohen, "Power Spectrum Analysis of Heart Rate Fluctuation: A Quantitative Probe of Beat - To - Beat Cardiovascular Control", *Science*, vol. 213, no. 4504, pp. 220-222, 1981.

[26]Y. Kuriyagawa and I. Kageyama, "A Modeling of Heart Rate variability to Estimate Mental Work Load", *IEEE International Conference on Systems, Man and Cybernetics*, vol. 2, 1999, pp. 294-299.

[27]D. R. Royall, E. C. Lauterbach, J. L. Cummings, A. Reeve, T. A. Rummans, D. I. Kaufer, W. C. LaFrance and C. E. Coffey, "Executive control function: A review of its promise and challenges for clinical research", *Journal of Neuropsychiatry and Clinical Neurosciences*, vol. 14, no. 4, pp. 377-405, 2002.

[28]A. Gevins, M. E. Smith, L. McEvoy and D. Yu, "High-resolution EEG mapping of cortical activation related to working memory: effects of task difficulty, type of processing, and practice", *Cerebral Cortex*, vol. 7, no. 4, pp. 374-385, 1997.

[29]P. Luu and M. I. Posner, "Anterior cingulate cortex regulation of sympathetic activity", *Brain*, vol. 126, no. 10, pp. 2119-2120, 2003.

[30]M. E. Smith, A. Gevins, H. Brown, H. Karnik and R. Du, "Monitoring task loading with multivariate EEG measures during complex forms of human-computer interaction", *Human Factors*, vol. 43, no. 3, pp. 366-380, 2001.

[31]B. Lorenz and R. Parasuraman, "Human operator functional state in automated systems: The role of compensatory control strategies", in *Operator Functional State: The Assessment and Prediction of Human Performance Degradation in Complex Tasks*, G. R. L. Hockey, A. W. K. Gaillard and O. Burov, Eds., Amsterdam:IOS Press, pp. 224-237, 2003.

[32]P. Ren, A. Barreto, Y. Gao and M. Adjouadi, "Affective assessment of computer users based on processing the pupil diameter signal", in *2011 Annual International Conference of the IEEE Engineering in Medicine and Biology Society, EMBC*, 2011, pp. 2594-2597.

[33]F. Mokhayeri and M.-R. Akbarzadeh-T, "Mental Stress Detection Based on Soft Computing Techniques", in *2011 IEEE International Conference on Bioinformatics and Biomedicine (BIBM)*, 2011, pp .430-433.

[34]J. Zhai, A. Barreto, C. Chin, C. Li, "Realization of stress detection using psychophysiological signals for improvement of human-computer interactions", in *Proceedings of the IEEE SoutheastCon*, 2005, pp. 415-420.

[35]L. A. Zadeh, "The Concept of a Linguistic Variable and its Application to Approximate Reasoning-I", *Information Sciences*, vol. 8, pp. 199-249, 1975.

[36]J. M. Mendel, "Type-2 Fuzzy Sets and Systems: An Overview [corrected reprint]", *IEEE Computational Intelligence Magazine*, vol. 2, no. 2, pp. 20-29, May 2007.

[37]J. M. Mendel and R. I. B. John, "Type-2 fuzzy sets made simple", *IEEE Transactions on Fuzzy Systems*, vol. 10, no. 2, pp. 117-127, Apr. 2002.

[38]L. A. Lucas, T. M. Centeno and M. R. Delgado, "General Type-2 Fuzzy Inference Systems: Analysis, Design and Computational Aspects", *IEEE International Fuzzy Systems Conference*, 2007, pp. 1-6.

[39]N. Sahab and H. Hagras, "Adaptive Non-singleton Type-2 Fuzzy Logic Systems: A Way Forward for Handling Numerical Uncertainties in Real World Applications", *International Journal of Computers, Communications & Control*, vol. 6, no. 3, pp. 503-529, Sep. 2011.

[40]N. N. Karnik, J. M. Mendel and Q. Liang, "Type-2 fuzzy logic systems", *IEEE Transactions on Fuzzy Systems*, vol. 7, no. 6, pp. 643-658, Dec. 1999.

[41]T. John and S. Coupland, "Type-2 Fuzzy Logic: Challenges and Misconceptions [Discussion Forum]", *IEEE Computational Intelligence Magazine,* vol. 7, no. 3, pp. 48-52, Aug. 2012.

[42]S. Coupland and R. John, "A Fast Geometric Method for Defuzzification of Type-2 Fuzzy Sets", *IEEE Transactions on Fuzzy Systems*, vol. 16, no. 4, pp. 929-941, Aug. 2008.

[43]Q. Liang and J. M. Mendel, "Interval type-2 fuzzy logic systems: theory and design", *IEEE Transactions on Fuzzy Systems*, vol. 8, no. 5, pp. 535-550, Oct. 2000.

[44]D. Wu and M. Nie, "Comparison and practical implementation of type-reduction algorithms for type-2 fuzzy sets and systems", in *2011 IEEE International Conference on Fuzzy Systems*, 2011, pp. 2131-2138.

[45]J. C. Bezdek, R. Ehrlich and W. Full, "FCM: The fuzzy c-means clustering algorithm", *Computers and Geosciences*, vol. 10, pp. 191-203, 1984.

[46]L. P. Kaelbling, M. L. Littman and A. W. Moore, "Reinforcement Learning: A Survey", *Journal of Artifical Intelligence Research*, vol. 4, pp. 237-285, 1996.

This article has been accepted for publication in a future issue of this journal, but has not been fully edited. Content may change prior to final publication. Citation information: DOI 10.1109/TFUZZ.2016.2598363, IEEE Transactions on Fuzzy Systems

Luis A. Torres Salomao (M'09) was born in Morelia, Mexico in 1986. He received the Bachelor Degree in electronic engineering from the UMSNH, Morelia, in 2009 and the Master of Science and Technology from the CIDESI in 2012. He is currently in the last year of his PhD studies at the Sheffield University Department of ACSE. His research interests include fault diagnosis, intelligent control systems, wind power, biomedicine and psycho-physiology.

Mahdi Mahfouf received the MPhil and PhD Degrees from the University of Sheffield, Sheffield, UK, in 1987 and 1991, respectively. He has held a Personal Chair in Intelligent Systems Engineering at the University of Sheffield since 2005. Professor Mahfouf is the author of more than 300 papers and has authored/co-authored one book and five book chapters. He has been working in the areas of Intelligent Systems Modelling, Optimization and Control in biomedicine as well as industrial systems for more than 30 years.

Emad El-Samahy was born in Cairo, Egypt, in 1970. He received the Bachelor and the MSc Degrees from the Military Technical College, Cairo, Egypt in 1992 and 1998 respectively. He received his PhD in Biomedical Engineering from the Sheffield University Department of ACSE in 2003. He is the author/coauthor of 20 articles and 2 book chapters. His research interests include biomedical modeling, intelligent control systems, psycho-physiology and exercise physiology.

Ching-Hua Ting received the MSc (Distinction in Control Systems) and PhD Degrees from the University of Sheffield, Sheffield, UK, in 1993 and 1999, respectively. He is currently a Professor and the Head of the Department of Mechanical and Energy Engineering, National Chiayi University, Chiayi, Taiwan. His research interests include bio-signal processing and bio-feedback control, monitoring and control of food processes, and industrial application of green energy.